

Referee 1:

Terms IVOC, LVOC, SVOC, etc. are used multiple times (e.g. p. 17299, Fig. 1) but are not defined here (definitions are provided in Donahue et al., 2012). I suggest providing a brief definition/description of these terms.

*We have added a description in the caption of Figure 1.*

Figure captions, especially figures 2-6, tend more towards discussion than description. I would suggest adding a sentence at the beginning of each to describe what is being plotted.

*We have added additional descriptions to Figures 2-6.*

Specific Comments:

p. 17292 Eq. 2: Do  $n_c$  and  $n_o$  correspond to the number of carbons and oxygens, respectively? *Yes. We have added an explanation of these terms after the equation.*

p. 17298 lines 6-7: Is there atmospheric relevance to values of 1 and 0.15, e.g. typical rural and urban values?  *$NO_x$  concentrations in remote areas can be as little as 2-8 ppt, while concentrations in urban areas range from 10-1000 ppb (Seinfeld and Pandis, 2006). This creates a range of  $\beta$  from 1 (where essentially none of the  $RO_2$  radicals are removed by  $NO$ ) to 0 (where essentially all of the  $RO_2$  radicals are removed by  $NO$ ), respectively.*

Fig 2: I assume the blue lines for OM are for high- $NO_x$  conditions and would suggest indicating this on the legend. *We have added a sentence clarifying this in the caption of the figure.*

Fig 3: Suggest noting in the caption the order of magnitude difference in the COM scales between plots (a) and (b). *We added a sentence in the caption noting the order of magnitude difference.*

Technical Corrections:

p. 17285 line 4: etc. Organics *Corrected*

p. 17285 line 25: organic compounds *Corrected*

p. 17286 line 11:  $NO_3$  has not [been] defined *We have added the definition in the previous paragraph.*

p. 17286 lines 17-18: most commonly *Corrected*

p. 17287 line 27: 30:46 can *Corrected*

p. 17291 line 4: MATLAB (throughout) *Corrected*

p. 17296 line 9: phase (Trump and Donahue, 2014), *Corrected*

p. 17296 line 15: left to a later *Corrected*

p. 17297 line 22: A concentration of  $100 \mu g m^{-3}$  *Corrected*

Referee 2:

Page 17289, Line 22: I think the VBS approach needs more than 4-7 species to be transported in 3-D air quality models. The number of advected species in 3D models depends on the implementation of the VBS approach, nevertheless at least 10-20 species are needed to be transported for implementation of the VBS approach in air quality models.

*A species here denotes a representative species for a single volatility bin. A basis set that uses 6 volatility bins would have 6 surrogate species. Depending on the implementation of the VBS, a 3-D model may use multiple instances of a basis set. Each instance can represent a different aerosol class or source. For instance, Koo et al. (2014) implements 5 species in its basis set each for SV-OOA, HOA, and BBOA. Using the 2D-VBS, the modeling of organics can be written as a single accumulation of mass regardless of source, or it can be treated separately.*

Equation 7: How much POA do you assume in your calculations?

*The model simulates a chamber experiment of  $\alpha$ -pinene aging and does not contain POA.*

In your calculations OH levels do not change depending on the NO<sub>x</sub> levels, right? Doesn't this introduce inconsistencies when the model is applied to ambient conditions? The same is true for other species, the 2D VBS model doesn't take into account chemical reactions between gaseous species. One of the ultimate goals of such detailed box modeling studies is to improve the SOA parametrization in air quality and climate models. My main comment is how one can use the findings of this updated 2D VBS box model in air quality models for SOA? I suggest authors to add estimates for sensitivity of SOA yields to NO<sub>x</sub> levels for major SOA precursors, e.g. toluene, long chain alkanes, terpenes etc. How the branching ratio calculation introduced by Lane et al. (2008) can be improved by using the results of this study? Since the full implementation of the 2D VBS approach in 3D models is not feasible due to the very high number of species that need to be tracked, the authors should provide some guidelines how such complex and detailed SOA models could be applied in more simplified SOA parametrizations, which are currently used in a number of air quality and climate models.

*A 3-D model is not the only case where the VBS is useful. This model is concerned with simulating the specific chemistry of  $\alpha$ -pinene aging that is studied in chamber experiments. During these experiments, the levels of reactants are held constant to understand the sophisticated chemistry that organic precursors undergo to form SOA. Thus, we are not making any statements about ambient concentrations of NO<sub>x</sub>, and the exploration of NO<sub>x</sub> on other organics is beyond the scope of this work. The next step in modeling more computationally intensive chemistry is Lagrangian plume tracking. This was first*

*implemented in PMCAMx by Murphy et al. (2012) to model the EU-CAARI campaigns. It has also been used in CMAQ by Koo et al. (2014) and Zhao et al. (2015).*

## References

- Koo, B., Knipping, E., and Yarwood, G.: 1.5-Dimensional volatility basis set approach for modeling organic aerosol in CAMx and CMAQ, *Atmos. Environ.*, 95, 158–164, doi:10.1016/j.atmosenv.2014.06.031, 2014.
- Murphy, B. N., Donahue, N. M., Fountoukis, C., Dall’Osto, M., O’Dowd, C., Kiendler-Scharr, A., and Pandis, S. N.: Functionalization and fragmentation during ambient organic aerosol aging: application of the 2-D volatility basis set to field studies, *Atmos. Chem. Phys.*, 12, 10 797–10 816, doi:10.5194/acp-12-10797-2012, 2012.
- Seinfeld, J. H. and Pandis, S. N.: *Atmospheric Chemistry and Physics: From Air Pollution to Climate Change*, Second Edition, John Wiley & Sons, Inc., 2006.
- Zhao, B., Wang, S., Donahue, N. M., Chuang, W., Hildebrandt Ruiz, L., Ng, N. L., Wang, Y., and Hao, J.: Evaluation of One-Dimensional and Two-Dimensional Volatility Basis Sets in Simulating the Aging of Secondary Organic Aerosol with Smog-Chamber Experiments, *Environ. Sci. Technol.*, 49, 2245–2254, doi:10.1021/es5048914, 2015.

List of changes:

1. page 1, line 42: Changed ellipsis to period after “such as nickel, manganese, etc”.
2. page 1, line 72: Change “organic compound” to “organic compounds”.
3. page 1, line 73: Added “(NO<sub>3</sub>)” after “nitrate”.
4. page 1, line 101: Changed “mostly” to “most”.
5. page 3, line 65: Changed “Matlab” to “MATLAB”.
6. page 4, line 17-18: Added “where  $n_C$  and  $n_O$  correspond to the number of carbon and oxygen atoms, respectively.”
7. page 4, line 26-27: The estimated parameter is  $\frac{1}{4}$ . Citation is accordingly changed.
8. page 4, line 54: Changed “Matlab” to “MATLAB”.
9. page 5, line 62: Changed position of comma to come after the citation.
10. page 5, line 70: Added “to” after “That is left...”
11. page 6, line 14-15: Add “A concentration of” before “100  $\mu\text{g m}^{-3}$ ”.
12. page 8, line 41: Changed “Matlab” to “MATLAB”.
13. Figure 1 caption, line 2: Add “The volatility space is divided into regions of organic compounds: extremely low volatility (ELVOC), low volatility (LVOC), semi-volatile (SVOC), intermediate volatility (IVOC), and volatile (VOC).”
14. Figure 2 caption, line 1: Add “Organic mass concentration over 2 hours of dark ozonolysis followed by 10 hours of OH aging for low-NO<sub>x</sub> and high-NO<sub>x</sub> conditions. The OM for non-nitrates and organonitrates plots are under high-NO<sub>x</sub> conditions.”
15. Figure 3 caption: Change caption to: “Mass of first generation products for each cell in the 2D-VBS, from 100  $\mu\text{g m}^{-3}$   $\alpha$ -pinene + ozone at  $\beta = 0.15$ . (a) total mass of all (organonitrate and non-nitrate) organics in both the suspended and vapor phases. (b) total mass of all organics in only the suspended phase. The suspended phase concentration axis is 2 orders of magnitude smaller than the vapor phase; most of the first generation mass remains in the vapor phase.”
16. Figure 4 caption: Change caption to: “The effect of peroxy-radical branching on the first-generation secondary organic aerosol concentration,  $C_{OM}$ . The x axis is the branching ratio for RO<sub>2</sub> reaction ( $\beta$ ), where  $\beta=1$  corresponds to low-NO<sub>x</sub> conditions dominated by RO<sub>2</sub> + HO<sub>2</sub> and  $\beta=0$  corresponds to high-NO<sub>x</sub> conditions dominated by RO<sub>2</sub> + NO. The y axis is

the ratio of  $C_{\text{OM}}$  at a given value of  $\beta$  to the low- $\text{NO}_x$  value. Each curve represents a different amount of oxidized precursor, spanning 5 orders of magnitude from  $10^2$  to  $10^6 \mu\text{g m}^{-3}$ .”

17. Figure 5 caption: Change caption to: “The effect of peroxy-radical branching on the aged secondary organic aerosol concentration,  $C_{\text{OM}}$  after 10 hours of oxidation by  $10^7 \text{OH cm}^{-3}$ . As in Fig. 4 the x axis is the branching ratio for  $\text{RO}_2$  reaction ( $\beta$ ), where  $\beta=1$  corresponds to the low- $\text{NO}_x$  conditions dominated by  $\text{RO}_2 + \text{HO}_2$  and  $\beta=0$  corresponds to high- $\text{NO}_x$  conditions dominated by  $\text{RO}_2 + \text{NO}$ . The y axis is the ratio of  $C_{\text{OM}}$  at a given value of  $\beta$  to the low- $\text{NO}_x$  value. Each curve represents a different amount of oxidized precursor, spanning 5 orders of magnitude from  $10^2$  to  $10^6 \mu\text{g m}^{-3}$ .”
18. Figure 6 caption, line 1: Change first sentence to: “The distribution of mass is plotted over the 2D-VBS space for multi-generation products, after 10 hours of OH aging of  $100 \mu\text{g m}^{-3}$   $\alpha$ -pinene + ozone at  $\beta = 0.15$ .”

**Abstract.** When  $\text{NO}_x$  is introduced to organic emissions, aerosol production is sometimes, but not always, reduced. Under certain conditions, these interactions will instead increase aerosol concentrations. We expanded the two-dimensional volatility basis set (2D-VBS) to include the effects of  $\text{NO}_x$  on aerosol formation. This includes the formation of organonitrates, where the addition of a nitrate group contributes to a decrease of 2.5 orders of magnitude in volatility. With this refinement, we model outputs from experimental results, such as the atomic N:C ratio, organonitrate mass, and nitrate fragments in AMS measurements. We also discuss the mathematical methods underlying the implementation of the 2D-VBS and provide the complete code in the supplemental material. A developer version is available on Bitbucket, an online community repository.

## 1 Introduction

Aerosols, or particulate matter (PM), cause numerous cardiovascular and respiratory diseases, and chronic exposure to high concentrations can significantly reduce life expectancy (Dockery et al., 1993; Peng et al., 2005; Pope et al., 2009). Particles smaller than 2.5 micrometers ( $\text{PM}_{2.5}$ ) directly contribute to respiratory- and cardiovascular-related deaths. This is most concerning in major cities where air pollution can reach extremely hazardous levels. In addition, PM affects ecosystems and the atmosphere, exerting significant direct and indirect forces on climate. Direct forcing comes from the scattering or absorption of solar radiation by aerosols. Indirect forcing comes from the scattering of solar radiation by clouds, which is in turn controlled by hydrophilic particles known as Cloud Condensation Nuclei (CCN) (Seinfeld and Pandis, 2006). In order to track the production of aerosols, models predict the interactions between emissions from various sources and their effects on the formation of PM.

$\text{PM}_{2.5}$  consists of a rich mixture including both inorganic and organic compounds, commonly found within individual particles. Inorganics include sodium chloride (from sea spray), sulfate (mostly from coal combustion), nitrate (mostly from high-temperature combustion), ammonium (from animal husbandry), elemental carbon (from combustion of organic fuels), and trace metals such as nickel, manganese, etc. Organics comprise 20-50% of  $\text{PM}_{2.5}$  mass in the continental mid-latitudes and as much as 90% in tropical forests (Andreae and Crutzen, 1997; Kanakidou et al., 2005). The organics are called organic aerosol (OA), and while the inorganics consist of a relatively small set of compounds, OA consists of a rich mixture containing many thousands of different individual organic compounds (Goldstein and Galbally, 2007; Kroll et al., 2011).

OA comes from biogenic (naturally-occurring) and anthropogenic (human-related) sources. Biomass burning (BBOA) is the largest contributor to OA worldwide (Bond

et al., 2004). Some BBOA comes from natural carbon (woodsmoke), but the combustion is largely associated with human activity and so BBOA is classified as anthropogenic. Overall, OA comprises roughly 10% of the total flux of organic carbon into (or out of) the atmosphere (Goldstein and Galbally, 2007; Hallquist et al., 2009); thus only a fraction of organic compounds have the right properties to reside in the condensed phase. The requisite property is a low volatility (Pankow, 1994; Donahue et al., 2011, 2014); to stay in the organic phase under typical conditions, an organic molecule must have a vapor pressure lower than roughly  $10^{-10}$  atm ( $10^{-5}$  Pa,  $C^* < 1 \mu\text{g m}^{-3}$ ) (Donahue et al., 2011).

OA is also classified as primary or secondary (Murphy et al., 2014; Cronn et al., 1977; Turpin and Huntzicker, 1995). Primary organic aerosols (POA) are directly emitted into the atmosphere on particles, and are largely from anthropogenic sources such as automobile exhaust and biomass burning. Secondary organic aerosols (SOA) are formed when chemical reactions cause condensation of organic compounds from the gas phase. Oxidants include ozone, hydroxyl ( $\text{OH}\cdot$ ) radicals, and nitrate ( $\text{NO}_3$ ) radicals (Turpin et al., 2000), and oxidation can occur in the gas phase (Pandis et al., 1991) or in the aqueous phase (Turpin et al., 2000). Oxidation can add functional groups to an organic backbone (functionalization), forming products with a lowered volatility; however, oxidation can also lead to C-C bond cleavage (fragmentation), often forming products with an elevated volatility (Kroll et al., 2011; Chacon-Madrid et al., 2010). In addition, association reactions between relatively volatile reaction products can lead to higher molecular weight, lower vapor pressure products (oligomers) (Kalberer et al., 2004).

Oxidation of an organic compound, even one generation, generally forms many products, each with a different volatility (Atkinson et al., 1997; Aumont et al., 2005; Lim and Ziemann, 2009). Thus SOA production has been described in terms of a volatility distribution of reaction products (Odum et al., 1996; Presto and Donahue, 2006; Donahue, 2012). However, this also means that the oxidation products (and thus volatility distribution and overall SOA mass yields) often depend strongly on ambient conditions. The dominant oxidant can have a large effect (OH vs ozone during the day,  $\text{NO}_3$  vs ozone at night), but so can the organic radical chemistry following the initial oxidation step.

One notable source of variability in SOA mass yields is the  $\text{NO}_x$  level (Presto and Donahue, 2006; Zhang et al., 2006; Ng et al., 2007; Logan et al., 1981; Thompson and Cicerone, 1982).  $\text{NO}_x$  (NO and  $\text{NO}_2$ ) can react with organic radicals to change the product distribution from oxidation reactions (Atkinson et al., 1997).  $\text{NO}_x$  is mostly-most commonly formed under high-temperature conditions such as combustion;  $\text{NO}_x$  concentrations range from 10-1000 ppb in urban areas to 10 ppt in remote regions (Seinfeld and Pandis, 2006), and so  $\text{NO}_x$  is one of the most highly variable reactive trace species in the atmosphere and also one of the most potent indications of human activity. Because  $\text{NO}_x$  can alter the

oxidation chemistry of organic compounds, even biogenic organic precursors (e.g. isoprene and terpenes) may in fact form “anthropogenically enhanced” SOA if the SOA mass yields are in some way enhanced by the presence of  $\text{NO}_x$ .

There is evidence that a large source of SOA associated with CO emissions (and thus presumably anthropogenic activity) is required to explain global surface OA observations (de Gouw and Jimenez, 2009; Spracklen et al., 2011). At the same time, a large fraction of OA appears to consist of modern carbon (containing  $^{14}\text{C}$ ) (Weber et al., 2007; Aiken et al., 2010; Minguillón et al., 2011; Zhang et al., 2012). This has led to speculation that interactions between biogenic precursors and urban plumes – possibly  $\text{NO}_x$  – may be responsible for the anthropogenic enhancement (Shilling et al., 2013). If so, the dramatic decline in  $\text{NO}_x$  levels in the southeast United States over the past decade (Russell et al., 2012) might be associated with a corresponding decrease in anthropogenically enhanced SOA.

Tracking any  $\text{NO}_x$  effect is thus extremely important. If changed product distributions (and thus SOA mass yields) were the sole effect of increased  $\text{NO}_x$ , then the  $\text{NO}_x$  influence could be dealt with easily by adjusting SOA mass yields based on  $\text{NO}_x$  levels (Presto and Donahue, 2006; Lane et al., 2008a). However, if there is a reason to track specific products, or if the subsequent, later-generation chemistry of the reaction products also differs substantially under high- and low- $\text{NO}_x$  conditions, then simply adjusting mass yields will not suffice. In the case of  $\text{NO}_x$ , both of these conditions apply: there is strong evidence that the aging chemistry of SOA depends on its composition (Zhang et al., 2006; Henry and Donahue, 2012), and also that organonitrates produced under high- $\text{NO}_x$  conditions are independently measured as a diagnostic of ambient aging conditions.

High organonitrate concentrations are typically found in areas with high  $\text{NO}_x$  levels. (Garnes and Allen, 2002; Mylonas et al., 1991) The addition of a nitrate functional group to a carbon backbone reduces volatility by  $\sim 2.5$  orders of magnitude (Pankow and Asher, 2008), potentially contributing to SOA formation as a result. Organonitrates can be identified on filter samples by characteristic absorption features using FTIR (Russell et al., 2011) and also in bulk mass spectra from the Aerosol Mass Spectrometer (AMS, Aerodyne Inc.) (Zhang et al., 2006; Farmer et al., 2010). Detection in the AMS is challenging because organonitrates fragment almost completely to give  $\text{NO}^+$  ( $m/z = 30$ ) and  $\text{NO}_2^+$  ( $m/z = 46$ ). The same fragments arise from (often much more abundant) inorganic nitrate; however, the fragment signal ratio (30:46) can be indicative of organonitrates and is quite distinct from ammonium nitrate (Farmer et al., 2010).

Depending on the carbon chain length, organonitrates can have a gas-phase atmospheric lifetime ranging from days to months, and thus drive long-range  $\text{NO}_x$  transport into remote marine regions (Atherton, 1989). Higher carbon number organonitrates will partition to the condensed phase (Ziemann and Atkinson, 2012). Organonitrates have been found

in aerosol samples at numerous sites across North America (Russell et al., 2011). In particular, high concentrations of organonitrates have been observed in California and Texas (Garnes and Allen, 2002; Day et al., 2010). AMS data from photooxidation of  $\alpha$ -pinene, limonene, and longifolene under high- $\text{NO}_x$  conditions show mass fragments corresponding to the formation of organonitrates (Zhang et al., 2006; Ng et al., 2007). In some field observations, roughly 10-20% of the organic aerosol mass is comprised of organonitrates; however, organonitrates are not always found in urban areas even in high- $\text{NO}_x$  conditions. Field data from Pittsburgh and the U.S. East Coast revealed low concentrations of aerosol organonitrates (Wittig et al., 2004; Russell et al., 2011). This may be due to the hydrolysis of organonitrates, where water reacts in the condensed phase with the nitrate group to form an alcohol and nitric acid (inorganic nitrate) (Liu et al., 2012). The change in the functional group likely has little effect on the volatility of the compound; the -OH functional group replacing the - $\text{ONO}_2$  group has about the same effect on volatility (Pankow and Asher, 2008).

During daytime, organonitrates are formed through reactions of NO with organic peroxy radicals ( $\text{RO}_2\cdot$ ). As  $\text{NO}_x$  concentrations rise, progressively more  $\text{RO}_2\cdot$  react with NO instead of  $\text{RO}_2\cdot$  or  $\text{HO}_2\cdot$ . The reaction with NO produces an intermediate product, ROONO, that can either decompose into an alkoxy radical ( $\text{RO}\cdot$  and  $\text{NO}_2$ ) or isomerize to form an organonitrate ( $\text{RONO}_2$ ) (Atkinson et al., 1997; Zhang et al., 2004). The alkoxy radicals will further react, either forming stable organics that are more functionalized or fragmenting to produce lower carbon-number products. Organonitrate yields from ROONO rise with carbon number and decreasing temperature and vary somewhat with structure, reaching an asymptotic limit of roughly 0.3 at 300K for most compounds relevant to SOA formation (Atkinson and Arey, 2003; Ziemann and Atkinson, 2012). Alkyl nitrates for species with  $>20$  carbons are predominantly in the particle phase (Lim and Ziemann, 2009). High- $\text{NO}_x$  products differ from low- $\text{NO}_x$  products; this can lead to comparatively higher or lower SOA concentrations (Presto et al., 2005; Kroll et al., 2006; Ng et al., 2007).

During nighttime, organonitrates are formed through reactions of  $\text{NO}_3$  with unsaturated organic precursors. (Crowley et al., 2011; Rollins et al., 2009) This reaction can produce organonitrates on the same magnitude as daytime organonitrate formation. (Fry et al., 2013) However, the concentration profile of  $\text{NO}_3$  is not well understood, and can vary widely depending on boundary layer conditions. (He et al., 2014; Fry et al., 2013) Daytime  $\text{NO}_3$  rapidly undergoes photolysis or reacts with NO to form  $\text{NO}_2$ , and are thus typically unable to form organonitrates in the presence of light. Product distributions for  $\text{NO}_3$  + VOC reactions have not been developed for the 2D-VBS, but its contribution to organonitrate production can eventually be incorporated within the current framework.

## 2 Background

### 2.1 Volatility Basis Set

The complexity of OA partitioning and the vast number of reaction products motivated the Volatility Basis Set (VBS). The original (one-dimensional) VBS was designed to represent partitioning and aging by lumping organic molecules only by volatility, in bins separated by an order of magnitude (at 300K) in a logarithmic volatility space (Donahue et al., 2006). That compact representation could describe SOA production and aging (Lane et al., 2008a) and also evaporation and subsequent aging of semi-volatile POA (Shrivastava et al., 2008) with 4-7 transportable surrogate species.

Aging schemes within the 1D-VBS employ a single coupling matrix (Donahue et al., 2006) that can vary with ambient conditions to represent changes in chemistry (Lane et al., 2008a). However, individual VBS bins can include such different species as  $C_{23}H_{48}$  (tricosane) and  $C_6H_{10}O_5$  (levoglucosan). There is good reason to believe that the chemistry of these species is quite different – most notably, fragmentation is likely to become more important with increasing oxygenation (Kroll et al., 2009, 2011). Furthermore, the degree of oxidation is an important diagnostic of ambient (Zhang et al., 2007; Jimenez et al., 2009) and chamber (Shilling et al., 2009; Chen et al., 2011) OA measurements. While fragmentation is described in the original 1D-VBS implementation (Donahue et al., 2006), the oxygen content is not tracked, cannot be used as a diagnostic, and cannot inform the aging chemistry.

The 2D-VBS adds a second dimension of oxygenation (O:C) or average carbon oxidation state ( $\overline{OS}_C = 2O:C - H:C$ ) (Donahue et al., 2011; Donahue, 2012). It was developed to capture these important defining properties of OA and track and predict changes over time.

The volatility and  $\overline{OS}_C$  of organic material are represented explicitly and evolve with aging chemistry, enabling explicit description of the production and evolution of SOA over time. In addition, rate constants for reactions with OH radicals are assigned based on typical chemical structures throughout the two-dimensional space (Donahue et al., 2013). While adding complexity, this expanded representation enables much more systematic exploration of different aging mechanisms in both box-models (Donahue, 2012) and Lagrangian chemical transport models (Murphy et al., 2012). It does not, however, enable explicit tracking of product categories such as organonitrates.

Here we describe a refinement to the 2D-VBS by introducing layers to hold key product classes – organonitrates in this case. This allows us to more accurately account for the effect of  $NO_x$  on the production and evolution of SOA and to capture a more complete picture of organic aging by incorporating the production and removal of organonitrates. The model replicates experimental data on the effect of  $NO_x$ , where high- $NO_x$  conditions increase SOA forma-

tion for certain precursors (longifolene) and decrease in others ( $\alpha$ -pinene) (Presto et al., 2005; Pathak et al., 2007; Kroll et al., 2006; Ng et al., 2007).

Mathematically, all implementations of the VBS are formally one-dimensional: an array of species is connected via a chemical coupling matrix that describes transformations due to aging reactions. However, the physical properties represented by that array of species can be cast into multiple dimensions – volatility, oxidation state, and now levels of key molecular classes. As part of the online supplemental material for this paper we have released a full implementation of the VBS, coded in [Matlab/MATLAB](#), providing full graphical diagnostics, access to the different levels of complexity (1D, 2D, layered), and instructions for alteration and expansion (e.g. changing volatility or oxidation state ranges, adding layers, etc.). In addition, more recent and updated versions of the code are stored in the online repository Bitbucket; instructions are detailed within the supplemental material.

### 2.2 Mathematical overview

The 2D-VBS follows the movement of carbon mass throughout the volatility and  $\overline{OS}_C$  space by modeling the basic aging processes of functionalization and fragmentation. Functionalization adds functional groups, producing more oxidized organics that have lower volatility than the parent compound. Fragmentation splits the carbon backbone of an oxidized compound, producing two smaller compounds of higher volatility and generally higher  $\overline{OS}_C$  (Donahue, 2012). The 2D-VBS implements these aging processes as a series of matrix manipulations.

While the 2D-VBS is typically presented as a two-dimensional space, it is implemented as a one dimensional concentration vector in the code.

The mass of carbon ( $C_{v,o}$ ) in  $\mu g m^{-3}$  is described in each cell ( $v, o$ ), where  $v$  is the volatility (x) index and  $o$  is the oxidation (y) index. This can be transformed into a single row vector  $C$  with  $n$  elements, or cells,  $n = v \times o$ . The transformation method concatenates the rows (the volatilities of each O:C) together:

$$\begin{bmatrix} C_{1,1} & \dots & C_{x,1} \\ \vdots & \ddots & \vdots \\ C_{1,y} & \dots & C_{x,y} \end{bmatrix} \rightarrow [C_{1,1} \dots C_{x,1} \ C_{1,2} \dots C_{x,2} \dots C_{1,y} \dots C_{x,y}] \quad (1)$$

The addition of dimensions, such as organonitrates, is implemented the same way by extending the one dimensional array to track these compounds.

Chemical reactions can then be represented as transformations from an initial cell  $i$  to all potential final cells  $f$ ; each transformation  $T$  is a column vector of length  $n$ , with  $\sum_f T_f = 1$  (the transformations conserve carbon). The  $n$  transformation vectors for each initial cell  $i$  can then be concatenated to form an  $n \times n$  transformation matrix,  $T =$



$[T_1 \dots T_n]$ . The overall chemical transformation is then given by  $\mathbf{C}\mathbf{T}$ .

The rate at which components react with OH (or any other oxidant) depends on their composition. Molecules with more carbons typically have more hydrogens available for abstraction reactions. Additionally, the more oxygens a molecule has, the more it is destabilized, and the more likely it will react. (Kwok and Atkinson, 1995) However, when enough functional groups become attached to the carbon backbone, the remaining hydrogen atoms are typically less reactive, and so reactivity decreases. A composition-activity relationship from (Donahue et al., 2013) accounts for these factors and is used to approximate rate constants gas-phase reactivity for each cell in the VBS. These values form a gas-phase reactivity vector,  $\mathbf{k}^{\text{vap}}$ :

$$\mathbf{k}^{\text{vap}} \simeq 1.2 \times 10^{-12} (n_C + 9n_O - 10(\text{O}:\text{C})^2) \text{cm}^3 \text{molec}^{-1} \text{s}^{-1} \quad (2)$$

where  $n_C$  and  $n_O$  correspond to the number of carbon and oxygen atoms, respectively.

We also parametrize the chemistry following the initial reaction with OH. The probabilities of fragmentation and functionalization are represented by vectors  $\mathbf{f}^{\text{frag}}$  and  $\mathbf{f}^{\text{func}}$ , respectively, where  $\mathbf{f}^{\text{frag}} = (\text{O}:\text{C})^n$  and  $\mathbf{f}^{\text{func}} = 1 - \mathbf{f}^{\text{frag}}$ . The formula for the potential for fragmentation is determined by the higher likelihood of fragmentation when a molecule is highly oxidized, because of the destabilizing effect of functional groups on the carbon backbone. The exponent,  $n$ , expresses the strength of fragmentation reactions, and is currently estimated to be  $\frac{1}{6}$  (Murphy et al., 2012)  $\frac{1}{4}$  (Donahue et al., 2012).

Functionalization kernels are created using a distribution based on the degree of oxidation of the compound. The kernel is defined in terms of a probability distribution for added oxygen and decreased volatility. (Donahue et al., 2012) That distribution is then mapped onto the  $C^o$ , O:C space to form a functionalization transformation array. For each volatility cell  $i$ , functionalization ( $\mathbf{T}_i^{\text{func}}$ ) distributes carbon mass throughout the  $n$  VBS cells.

Fragmentation kernels describe the distribution of organic material throughout (mostly) higher volatility bins and O:C following cleavage of the carbon backbone. Some fragmentation products are molecules and some are radicals, which in turn are rapidly functionalized; the fragmentation kernel describes the ultimate distribution of stable products from this process and thus distributes carbon over a much wider range of the VBS than functionalization. (Donahue et al., 2012) The overall transformation vector  $\mathbf{T}_i$  is found for functionalization and fragmentation by combining the two processes together,  $\mathbf{T}_i = \mathbf{f}_i^{\text{frag}} \cdot \mathbf{T}_i^{\text{frag}} + \mathbf{f}_i^{\text{func}} \cdot \mathbf{T}_i^{\text{func}}$ . Also,  $\sum_{f=1}^n T_{i,f} = 1$ , meaning carbon mass is conserved. Concatenated over all columns,  $i = 1 \dots n$ , the transformations form the transformation matrix  $\mathbf{T}$ . The aging process is then ex-

pressed as:

$$\frac{\partial \mathbf{C}}{\partial t} = \mathbf{k}^{\text{vap}} \cdot [\text{OH}] \cdot \mathbf{C}(\mathbf{T} - \mathbf{I}) \quad (3)$$

This can be modeled with differential solvers in [Matlab](#) [MATLAB](#).

The transformations just described apply to species in the vapor phase. The VBS separately tracks vapor ( $\mathbf{C}^{\text{vap}}$ ) and condensed ( $\mathbf{C}^{\text{cond}}$ ) phase concentrations. For the condensed phase, the OH rate constant is specified as an effective gas-phase rate constant,  $k_i^{\text{eff}}$ , which is determined by the diffusion-limited uptake of gas-phase OH by particles, based on the Fuchs corrected surface area of a given particle size distribution (Donahue et al., 2013). We generally assume this is independent of composition and that OH reacts with unit efficiency once it reaches the surface of a particle. Lacking other constraints, we assume that  $\mathbf{f}^{\text{func}}$  and  $\mathbf{f}^{\text{frag}}$  are the same in the gas and condensed phases, so  $\mathbf{T}^{\text{vap}} = \mathbf{T}^{\text{cond}}$ ; however, it is likely that even the functionalization and fragmentation kernels differ in the gas and condensed phases, so we anticipate that future refinements will remove this assumption.

Additional details on the distribution of material throughout the VBS may be found in Donahue et al. (2012) and Murphy et al. (2012).

### 2.3 Treatment of Organonitrates

The introduction of  $\text{NO}_x$  to the system brings additional chemical reactions and the potential to form organonitrates through the functionalization process. Organonitrates are accounted for in a separate layer of the 2D-VBS, called the “N<sub>1</sub>” layer for the inclusion of an atomic nitrogen. The addition of a nitrate group decreases the volatility by  $\sim 2.5$  orders of magnitude (Pankow and Asher, 2008) and increases the number of oxygens attached to the carbon backbone by 1 (the other oxygen atoms and the nitrogen constitute an  $\text{NO}_2$  group).

This has the potential to produce high concentrations of organonitrates in the condensed phase because of the large decrease in the volatility of the product compared to the reactant.

The formation of an organonitrate involves two branch points. The first is the probability  $(1 - \beta)$  that  $\text{RO}_2$  will react with NO; the second is the yield,  $\eta$ , of organonitrates from  $\text{RO}_2 + \text{NO}$ . The nitrate yield  $\eta$  rises with increasing carbon number (Arey et al., 2001; Yeh and Ziemann, 2014) and depends on the functionality of the  $\text{RO}_2$  (Lim and Ziemann, 2009; Elrod, 2011); however, for organics large enough to partition to the condensed phase,  $\eta$  is at an asymptotic limit, and we assume a homogeneous distribution of  $\text{RO}_2$  structures within any given VBS cell. We thus assume that  $\eta = 0.30$  in all cases. Various ways of estimating  $\beta$  are possible, such as from the  $\text{VOC}:\text{NO}_x$  ratios obtainable in experimental data, (Presto et al., 2005) to the comparison of the rates of reaction

between  $\text{RO}_2 + \text{NO}$  and  $\text{RO}_2 + \text{HO}_2$ . (Lane et al., 2008b) In this work, we will simply vary  $\beta$  parametrically.

There are now three different transformation pathways for organics in the  $N_0$  (non-organonitrate) layer: they can fragment, functionalize without forming organonitrates, or form organonitrates. As a simplification, we assume that there are two pathways for organonitrates in the  $N_1$  layer: they can fragment by eliminating the  $\text{NO}_2$  group and return to the  $N_0$  layer, or they can functionalize and remain in the  $N_1$  layer. Also as a simplification we assume that dinitrates with 2  $-\text{ONO}_2$  functional groups are minor products, and so we do not add an  $N_2$  layer. The transformations for the organonitrate case are analogous to the non-organonitrate case, but with expansions to accommodate the production and loss of organonitrates. The concentration array doubles in size:  $\mathbf{C} = [\mathbf{C}_{N_0} \mathbf{C}_{N_1}]$ , where  $\mathbf{C}_{N_0}$  represents all the cells in the  $N_0$  layer and  $\mathbf{C}_{N_1}$  represents the cells in the  $N_1$  layer. More complex is the transformation matrix, which is now:

$$\mathbf{T} = \begin{bmatrix} \mathbf{T}_{N_0 \rightarrow N_0} & \mathbf{T}_{N_0 \rightarrow N_1} \\ \mathbf{T}_{N_1 \rightarrow N_0} & \mathbf{T}_{N_1 \rightarrow N_1} \end{bmatrix} \quad (4)$$

where:  $\mathbf{T}_{N_0 \rightarrow N_0}$  represents the original functionalization and fragmentation of the non-organonitrate layer.  $\mathbf{T}_{N_0 \rightarrow N_1}$  is the formation of an organonitrate through functionalization.  $\mathbf{T}_{N_1 \rightarrow N_0}$  is the fragmentation of an organonitrate.  $\mathbf{T}_{N_1 \rightarrow N_1}$  is the functionalization of an organonitrate. The organonitrate ( $N_1$ ) layer of the 2D-VBS contains only one nitrate group, and thus each species contains a single nitrogen atom. Because  $n_N$  is constant, N:C drops as volatility decreases and the chemical species become larger. In addition, the oxygen attached to the carbon from the nitrate group contributes to the O:C of the overall compound. Therefore, the O:C of an organonitrate can never be 0. Figure 1 shows N:C for the nitrate layer ( $N_1$ ) of the 2D-VBS. In the regime where aerosols tend to form under atmospheric conditions, N:C ranges from 0.04 to 0.3. Semi-volatile organonitrates have N:C from around 0.05 to 0.3; extremely low volatility compounds have an N:C lower than 0.2.

N:C for ambient aerosols are experimentally obtainable through Atomic Mass Spectroscopy (AMS). (Rollins et al., 2010) tested compounds that act as aerosol precursors in the atmosphere using the AMS, and the data from elemental analyses of these organic hydroxynitrates showed N:C ranging from 0.02 to 0.1. Other experiments of SOA production from isoprene, toluene, and naphthalene in high- $\text{NO}_x$  conditions show N:C ranging from .04 to .08, indicating the existence of low volatility compounds with moderate levels of oxygenation. (Chhabra et al., 2010) In addition to providing a sense of the range of N:C expected in aerosols, Figure 1 also reveals the relationship between N:C and the size of the molecule itself. Molecules with very small N:C actually indicate high carbon content, meaning these organonitrates are, on a per molecule basis, contributing significant mass to the overall organic aerosol.

## 2.4 Time evolution

Once the transformation matrix  $\mathbf{T}$  has been specified for any VBS configuration, the time evolution is trivially specified. A final detail is that we separate vapor-phase and particle-phase processes to treat the very different kinetics of homogeneous and heterogeneous oxidation. (Donahue et al., 2013) This also facilitates dynamical treatments of aerosol processes. (Trump et al., 2014; Trump and Donahue, 2014) We can also treat oligomerization within the condensed phase — (Trump and Donahue, 2014) (Trump and Donahue, 2014), though we shall not address that here. Formally, this again requires that we double the concentration array to distinguish vapor- and condensed-phase concentrations:  $\mathbf{C} = [\mathbf{C}^{\text{vap}} \mathbf{C}^{\text{cond}}]$ . The transformation matrix becomes:

$$\mathbf{T} = \begin{bmatrix} \mathbf{T}^{\text{vap}} & 0 \\ 0 & \mathbf{T}^{\text{cond}} \end{bmatrix} \quad (5)$$

This is block diagonal because we do not treat particle microphysics – condensation and evaporation – at this stage. That is left to a later step via operator splitting, whether we assume equilibrium partitioning or specifically treat the dynamics.

The change in the mass within each cell is described by  $n$  differential equations. For each cell  $i$  out of a total of  $n$  cells in the VBS,

$$\frac{d\mathbf{C}}{dt} = C_{\text{OH}} [(\mathbf{k} \cdot \mathbf{C}) \mathbf{T} - (\mathbf{k} \cdot \mathbf{C})] = C_{\text{OH}} (\mathbf{k} \cdot \mathbf{C}) [\mathbf{T} - \mathbf{I}] \quad (6)$$

where the first term is the amount of mass that is reacted into the cell from all other cells, and the second term is the loss from reactions out of the cell.

Any differential equation solver can be employed to solve Eq. 6. We currently use the approximation  $\exp(-k\Delta t) \approx 1 - k\Delta t$  for small  $\Delta t$ .

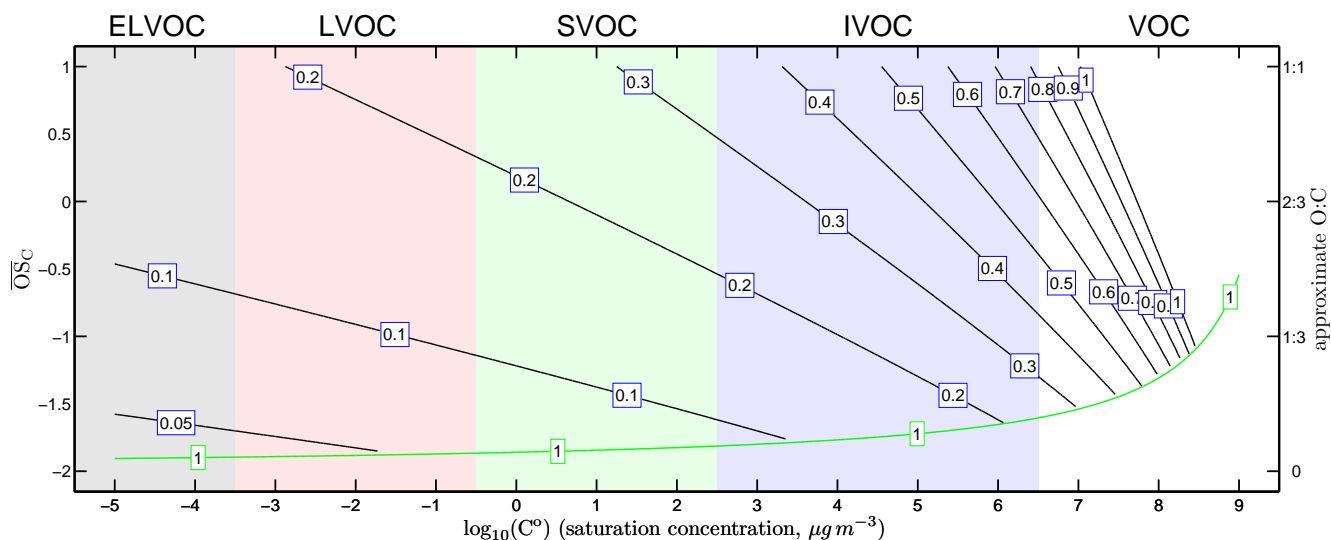
As functionalized products shift into lower volatility cells, they can condense into the aerosol phase. At equilibrium this is given by:

$$\xi_i = \left(1 + \frac{C_i^*}{C_{\text{OA}}}\right)^{-1}; \quad C_{\text{OA}} = \sum_i C_i^* \xi_i \quad (7)$$

where  $C^*$  is the volatility (in  $\mu\text{g m}^{-3}$ ) of the compound,  $\xi$  is the fraction of organics in the condensed phase, and  $C_{\text{OA}}$  is the total organic aerosol mass. This is a constant balancing act – if more functionalized material with lower volatility form and more mass condense, some higher volatility products will also condense. The reverse is also true – if fragmentation becomes dominant and higher volatility products form, lower volatility products may enter the vapor phase.

## 3 Results and Discussion

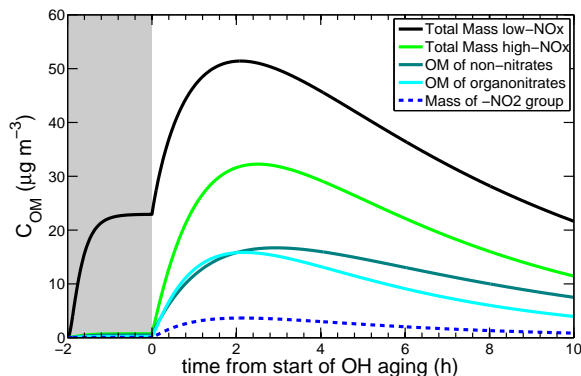
Prior VBS model implementations have treated ozonolysis and subsequent OH multi-generational aging of  $\alpha$ -pinene in



**Fig. 1.** Atomic N:C ratio isopleths in the organonitrate layer of the 2D-VBS. Broad volatility ranges are shown with the colored background. The volatility space is divided into regions of organic compounds: extremely low volatility (ELVOC), low volatility (LVOC), semi-volatile (SVOC), intermediate volatility (IVOC), and volatile (VOC). Most organonitrate aerosols will have an N:C ratio lower than 0.2. The green line represents the single oxygen isopleth under which no organonitrate exists, because organonitrates themselves contribute an oxygen to the O:C ratio.

chamber studies. A 2D-VBS model reproduced aerosol mass well throughout the course of the MUCHACHAS experiments, which studied SOA aging under similar conditions in four different chambers (Donahue et al., 2012). Building upon this, the current version (v1.0 in Bitbucket) of the 2D-VBS model can also model  $\alpha$ -pinene aging under high- $\text{NO}_x$  conditions with both ozonolysis aging and OH aging periods. While there are currently few high- $\text{NO}_x$  experimental data addressing multi-generational aging, mass yields of first-generation products from ozonolysis of  $\alpha$ -pinene are available (Pathak et al., 2007; Presto et al., 2005). Simulations for high- $\text{NO}_x$  cases are run based on this data.

In the examples shown, we run the model under ideal chamber conditions, where there are no wall losses. A concentration of  $100 \mu\text{g m}^{-3}$  of  $\alpha$ -pinene is introduced into the chamber. For the first two hours, we model dark conditions with a constant ozone level of 300 ppbv. The ozone reacts with the unsaturated carbon bonds to form first-generation products. At the end of two hours, after all of the precursor material has been reacted to form first-generation products, OH is introduced into the chamber at a constant  $10^7$  molecules  $\text{cm}^{-3}$  for 10 hours. This is the equivalent of turning on the UV lights in a chamber with a strong OH precursor such as HONO. The continued reaction of organic compounds creates multi-generational products, many of which are low volatility and condense into the aerosol phase. We have taken a low- and high- $\text{NO}_x$  case, where  $\beta = 1$  and  $\beta = 0.15$ , respectively, and examined the differences in aerosol production during first generation chemistry and subsequent multi-generational chemistry.



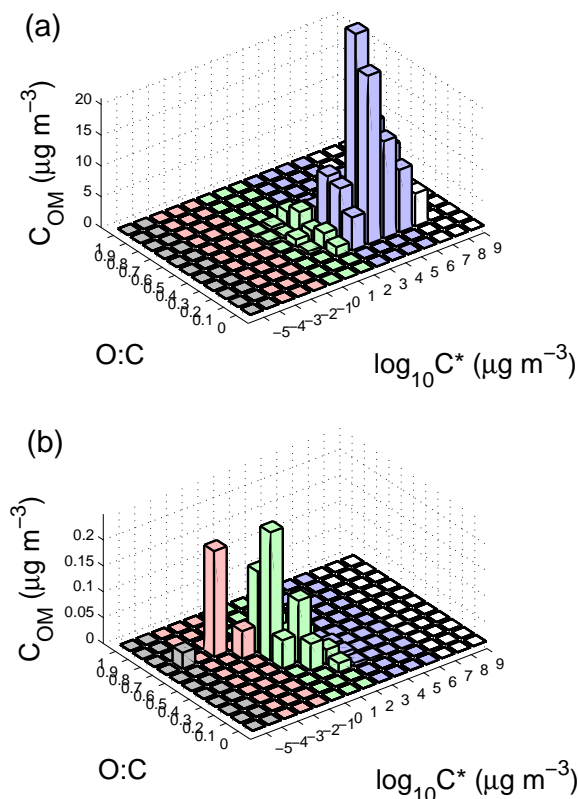
**Fig. 2.** Organic mass concentration over 2 hours of dark ozonolysis followed by 10 hours of OH aging for low- $\text{NO}_x$  and high- $\text{NO}_x$  conditions. The OM for non-nitrates and organonitrates plots are under high- $\text{NO}_x$  conditions. High- $\text{NO}_x$  conditions decrease the overall organic aerosol mass produced throughout the course of a model run. At  $\beta = 0.15$  (85%  $\text{RO}_2 + \text{NO}$ ), the mass concentration of organonitrates is roughly equivalent to the mass concentration of non-organonitrates. While the contribution of the  $-\text{NO}_2$  group itself is small, the organonitrate compounds can comprise a significant portion of the overall mass.

Figure 2 shows the differences in concentration of aerosol mass produced under low- and high- $\text{NO}_x$  conditions throughout the course of the chamber model run. During first generation chemistry, high- $\text{NO}_x$  conditions form very little aerosol mass, while low- $\text{NO}_x$  conditions produce high SOA

mass. This is due to higher volatility compounds that are generated because of the presence of  $\text{NO}_x$ , instead of the semi-volatile compounds in the absence of  $\text{NO}_x$ . When OH aging begins at low  $\text{NO}_x$ , the aerosol mass more than doubles as volatile compounds react to form highly functionalized, low volatility species. An even more dramatic effect is seen in the OH aging of high- $\text{NO}_x$  first generation compounds. While most first generation products were too volatile to condense, subsequent aging pushed a significant portion of these organics into the aerosol phase. Under these model conditions, even with the dramatic increase in concentration, the high- $\text{NO}_x$  condition produces less overall mass during OH aging. This alternate pathway results in a significant contribution by organonitrates to the overall aerosol mass – organonitrates comprised nearly half of the total organic mass at one point during OH aging. While the mass of organonitrates is significant, if the AMS were to test this sample, it would measure only a small concentration of N-containing mass fragments (indicated with the dashed blue curve in the figure). In essence, these are very large organonitrate molecules that have significant impact on overall aerosol mass.

The distribution of mass under high- $\text{NO}_x$  conditions offers insight into the low mass production during first generation aging. Figure 3 shows the first generation distribution (at  $t = 0$  of Figure 2) of organics when  $\beta = 0.15$ . This distribution is based on chamber experiments by Pathak et al. (2007) and Presto et al. (2005) of  $\alpha$ -pinene ozonolysis under high- $\text{NO}_x$  concentrations. Figure 3a shows the distribution of all organics (both aerosol and vapor phase). The majority of the organics reside in the IVOC range, which is too volatile to condense in the typical mass loadings of the atmosphere. Figure 3b shows the distribution of total suspended material, comprised of both organonitrates and non-nitrates. This mass contains more oxidized material than those in the vapor phase, and range from LVOC to SVOC. Compared to the first generation distribution in low- $\text{NO}_x$  conditions shown in Figure 2, the high- $\text{NO}_x$  condition produces less aerosol mass because of the overall higher volatilities of resulting compounds.

The previous figures have shown that the presence of  $\text{NO}_x$  decreases aerosol mass production for  $\alpha$ -pinene under moderate loadings. Less volatile precursors like sesquiterpenes are affected differently by  $\text{NO}_x$ . A precursor with a lower volatility than  $\alpha$ -pinene, such as longifolene, produces products with correspondingly lower volatility. (Ng et al., 2007) While first generation distributions for these precursors are currently lacking, we can emulate this effect by increasing the mass loading of  $\alpha$ -pinene instead. A precursor compound that is an order of magnitude less volatile than  $\alpha$ -pinene can be modeled by an order of magnitude increase in mass loading. Figure 4 shows a comparison of first generation aerosol concentration under various  $\beta$  and mass loadings to the mass concentration produced under low- $\text{NO}_x$ . This shows that for lower mass loadings of  $\alpha$ -pinene such as  $100 \mu\text{g m}^{-3}$ , increasing  $\text{NO}_x$  levels decreases resultant mass. As the load-



**Fig. 3.** First Mass of first generation products for each cell in the 2D-VBS, from  $100 \mu\text{g m}^{-3}$   $\alpha$ -pinene + ozone at  $\beta = 0.15$ . (a) total mass of all (organonitrate and non-nitrate) organics in both the suspended and vapor phases. (b) total mass of all organics in only the suspended phase. Most The suspended phase concentration axis is 2 orders of magnitude smaller than the vapor phase; most of the first generation mass remains in the vapor phase.

ings increase in magnitude, the aerosol suppression effect of  $\text{NO}_x$  decreases. When loadings reach  $10^5 \mu\text{g m}^{-3}$ , the effect is reversed, instead producing more mass as  $\text{NO}_x$  levels increase. This has been shown in experimental data from Ng et al. (2007), where longifolene exhibit higher yields under high- $\text{NO}_x$  conditions than low- $\text{NO}_x$  conditions. Even though the presence of  $\text{NO}_x$  produces first generation compounds from longifolene that are higher in volatility than first generation compounds produced under low  $\text{NO}_x$ , these compounds are still LVOCs and SVOCs, and partition into the aerosol phase. In addition, the organonitrate group contributes significant mass to the aerosol phase, resulting in the  $>1$  high- $\text{NO}_x$  to low- $\text{NO}_x$  organic mass ratio. Depending on the volatility of the organic precursor, it is therefore possible for the presence of  $\text{NO}_x$  to increase or decrease the total first generation aerosol mass.

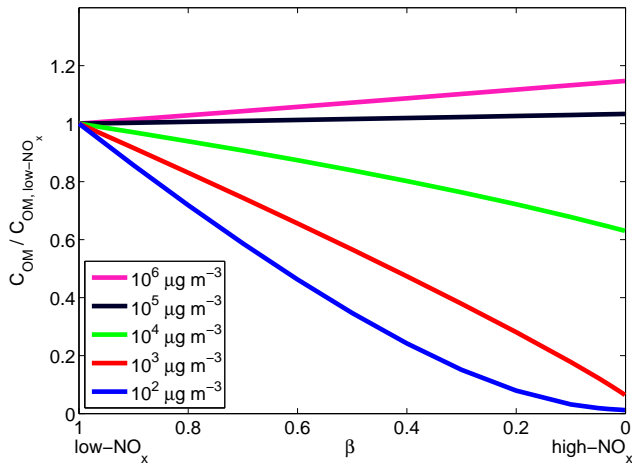


**Fig. 4.** For first generation yields at low precursor concentrations, increasing  $\text{NO}_x$  concentration decreases the effect of peroxy-radical branching on the first-generation secondary organic aerosol concentration,  $C_{\text{OM}}$ . This is analogous to the branching ratio for  $\text{RO}_2$  reaction ( $\beta$ ), where  $\beta=1$  corresponds to starting with low- $\text{NO}_x$  conditions dominated by  $\text{RO}_2 + \text{HO}_2$  and  $\beta=0$  corresponds to high- $\text{NO}_x$  conditions dominated by  $\text{RO}_2 + \text{NO}$ . The y axis is the ratio of  $C_{\text{OM}}$  at a high volatility precursor like  $\alpha$ -pinene given value of  $\beta$  to the low- $\text{NO}_x$  value. High volatility precursors result in higher aerosol levels, spanning 5 orders of magnitude from the  $-\text{ONO}_2$  group and lower volatility. Low volatility precursors such as longifolene has been shown to produce more aerosol under high- $\text{NO}_x$  conditions than under low- $\text{NO}_x$  conditions.

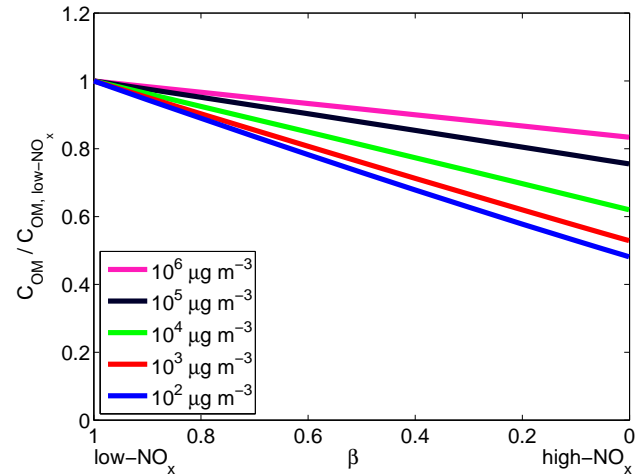


**Fig. 5.** After the effect of peroxy-radical branching on the aged secondary organic aerosol concentration,  $C_{\text{OM}}$  after 10 hours of oxidation by  $10^7 \text{ OH}$  aging, there is a smaller gap between different loadings under high- $\text{NO}_x$  conditions. The presence of  $\text{NO}_x$  also now consistently decreases  $C_{\text{OM}}$  at a given value of  $\beta$  to the total aerosol mass produced low- $\text{NO}_x$  value. Each curve represents a different amount of oxidized precursor, as opposed to spanning 5 orders of magnitude from  $10^2$  to increasing mass during first generation chemistry under high precursor loadings.

As these first generation products undergo multi-generational chemistry, becoming a more complex mix of organics, the stark differences between the mass loadings under first generation chemistry are dampened. Figure 5 shows the comparison between different  $\beta$  and different initial mass loadings with respect to the low- $\text{NO}_x$  ( $\beta = 1$ ) case, after 10 hours of OH aging. This corresponds to the end of the time period in Figure 2. While higher loadings continue to produce more aerosol mass, an increase in  $\text{NO}_x$  now consistently produces lower mass. This comes from the tendency to cleave the nitrate group during fragmentation, decreasing the effect of the nitrate group on overall mass. In addition, the probability of fragmentation increases as functionalization continues throughout the course of aging, contributing to the loss of organonitrates and the loss of aerosol mass to the vapor phase.

The distribution of suspended mass throughout the VBS also changes over the course of OH aging. Figure 6 shows the distribution of mass in the 2D-VBS for the organonitrate layer (Figure 6a) and the non-nitrate (Figure 6b) after 10 hours of OH aging. This corresponds to the endpoints of the “OM of organonitrates” and “OM of non-nitrates” lines in Figure 2. The organonitrate concentration is fairly small,

and they are only moderately oxidized, while the non-nitrate organics are highly oxidized. Each cell of the organonitrate layer, with higher mass yet lower carbon numbers, is slower to react compared to the corresponding cell in the non-nitrate layer. However, as the organonitrates undergo repeated functionalization, fragmentation of the products become more preferable, leaving behind less oxidized material in the organonitrate layer. Fragmentation of these highly functionalized organonitrates cleaves the nitrate group, resulting in highly oxidized non-nitrate organics. As a result, the organonitrate layer tends to be less oxidized and semi-volatile while non-nitrates are highly oxidized.

## 4 Conclusions

We have added a layer to the 2D-VBS to account for organonitrates. In addition, we have developed a module to treat the formation and aging of organonitrates under high- $\text{NO}_x$  conditions, and released a complete implementation of this code in [Matlab/MATLAB](#).

There are relatively few experimental constraints on the behavior of organonitrates in SOA, especially for multi-generational aging. Unknowns include differences between homogeneous and heterogeneous oxidation and the fate of

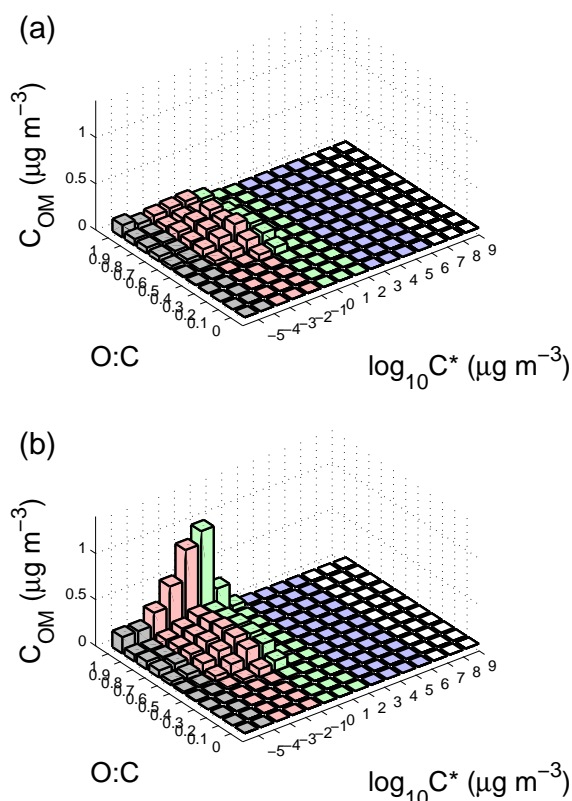


**Fig. 6. Multi-generation**—The distribution of mass is plotted over the 2D-VBS space for multi-generation products, after 10 hours of OH aging of  $100 \mu\text{g m}^{-3}$   $\alpha$ -pinene + ozone at  $\beta = 0.15$ . (a) the 1N layer, where the mass of products are highest in the moderately oxidized and semi-volatile ranges. (b) the 0N layer, where the mass is highly oxidized and lower in volatility.

nitrates after fragmentation. As a simplification we have assumed that homogeneous and heterogeneous product distributions are the same, and that fragmentation breaks the weakest bond in the organonitrate, assumed to be the O-NO<sub>2</sub> bond. However, it is certain that semi-volatile products (nitrate and non-nitrate alike) will react relatively rapidly in the gas phase and consequently that any first-generation semi-volatile products will not be long lived in the atmosphere.

We explored the aging chemistry of SOA under conditions typical of chamber experiments. During multi-generational aging under high-NO<sub>x</sub> conditions, the contribution of organonitrates to organic mass is similar to non-nitrate organics. This contribution of organonitrates to aerosol mass can be large even though the actual nitrate (-ONO<sub>2</sub>) mass is low, because the N:C of condensed-phase organonitrates can be low. We also reproduced the enhancement of aerosol

production in the presence of NO<sub>x</sub>, under conditions such as high mass loadings or low volatility precursors. This showed that the VBS is capable of accounting for these effects on extensive organic chemistry and emphasized the important role that NO<sub>x</sub> plays as part of the aging process.

*Acknowledgements.* This work was funded by the National Science Foundation, the EPA STAR program, and the Electric Power Research Institute (EPRI).

## References

- Aiken, A. C., De Foy, B., Wiedinmyer, C., Decarlo, P. F., Ulbrich, I. M., Wehrli, M. N., Szidat, S., Prévôt, A. S. H., Noda, J., Wacker, L., Volkamer, R., Fortner, E., Wang, J., Laskin, A., Shuthanandan, V., Zheng, J., Zhang, R., Paredes-Miranda, G., Arnott, W. P., Molina, L. T., Sosa, G., Querol, X., and Jimenez, J. L.: Mexico city aerosol analysis during MILAGRO using high resolution aerosol mass spectrometry at the urban supersite (T0)-Part 2: Analysis of the biomass burning contribution and the non-fossil carbon fraction, *Atmos. Chem. Phys.*, 10, 5315–5341, 2010.
- Andreae, M. O. and Crutzen, P. J.: Atmospheric Aerosols: Biogeochemical Sources and Role in Atmospheric Chemistry, *Science* (80-.), 276, 1052–1058, 1997.
- Arey, J., Aschmann, S. M., Kwok, E. S. C., and Atkinson, R.: Alkyl Nitrate, Hydroxyalkyl Nitrate, and Hydroxycarbonyl Formation from the NO<sub>x</sub> - Air Photooxidations of C5 - C8 n-Alkanes, *J. Phys. Chem. A.*, 105, 1020–1027, 2001.
- Atherton, C. S.: Organic nitrates in remote marine environments: Evidence for long-range transport, *Geophys. Res. Lett.*, 16, 1289–1292, 1989.
- Atkinson, R. and Arey, J.: Atmospheric degradation of volatile organic compounds., *Chem. Rev.*, 103, 4605–38, 2003.
- Atkinson, R., Baulch, D. L., Cox, R. A., Hampson, R. F., Kerr, J. A., Rossi, M. J., and Troe, J.: Evaluated Kinetic, Photochemical and Heterogeneous Data for Atmospheric Chemistry: Supplement V. IUPAC Subcommittee on Gas Kinetic Data Evaluation for Atmospheric Chemistry, *J. Phys. Chem. Ref. Data*, 26, 521 – 1011, 1997.
- Aumont, B., Szopa, S., and Madronich, S.: Modelling the evolution of organic carbon during its gas-phase tropospheric oxidation: development of an explicit model based on a self generating approach, *Atmos. Chem. Phys.*, 5, 2497–2517, 2005.
- Bond, T. C., Streets, D. G., Yarber, K. F., Nelson, S. M., Woo, J.-H., and Klimont, Z.: A technology-based global inventory of black and organic carbon emissions from combustion, *J. Geophys. Res.*, 109, 1–43, 2004.
- Chacon-Madrid, H. J., Presto, A. A., and Donahue, N. M.: Functionalization vs. fragmentation: n-aldehyde oxidation mechanisms and secondary organic aerosol formation., *Phys. Chem. Chem. Phys.*, 12, 13 975–13 982, 2010.
- Chen, X., Hopke, P. K., and Carter, W. P. L.: Secondary organic aerosol from ozonolysis of biogenic volatile organic compounds: chamber studies of particle and reactive oxygen species formation, *Environ. Sci. Technol.*, 45, 276–282, 2011.
- Chhabra, P. S., Flagan, R. C., and Seinfeld, J. H.: Elemental analysis of chamber organic aerosol using an aerodyne high-resolution

- aerosol mass spectrometer, *Atmos. Chem. Phys.*, 10, 4111–4131, 2010.
- Cronn, D. R., Charlson, R. J., Knights, R. L., Crittenden, A. L., and Appel, B. R.: A Survey Of The Molecular Nature Of Primary And Secondary Components Of Particles In Urban Air By High-Resolution Mass Spectrometry, *Atmos. Environ.*, 10, 929–937, 1977.
- Crowley, J. N., Thieser, J., Tang, M. J., Schuster, G., Bozem, H., Beygi, Z. H., Fischer, H., Diesch, J. M., Drewnick, F., Borrmann, S., Song, W., Yassaa, N., Williams, J., Pöhler, D., Platt, U., and Lelieveld, J.: Variable lifetimes and loss mechanisms for NO<sub>3</sub> and N<sub>2</sub>O<sub>5</sub> during the DOMINO campaign: Contrasts between marine, urban and continental air, *Atmos. Chem. Phys.*, 11, 10853–10870, 2011.
- Day, D. A., Liu, S., Russell, L. M., and Ziemann, P. J.: Organonitrate group concentrations in submicron particles with high nitrate and organic fractions in coastal southern California, *Atmos. Environ.*, 44, 1970–1979, 2010.
- de Gouw, J. and Jimenez, J. L.: Organic aerosols in the Earth's atmosphere., *Environ. Sci. Technol.*, 43, 7614–7618, 2009.
- Dockery, D. W., Pope, C. A., Xu, X., Spengler, J. D., Ware, J. H., Fay, M. E., Ferris, B. G., and Speizer, F. E.: An Association Between Air Pollution and Mortality in Six Cities, *N. Engl. J. Med.*, 329, 1753–1759, 1993.
- Donahue, N. M.: A two-dimensional volatility basis set - Part 2: Diagnostics of organic-aerosol evolution, *Atmos. Chem. Phys.*, 12, 615–634, 2012.
- Donahue, N. M., Robinson, A. L., Stanier, C. O., and Pandis, S. N.: Coupled partitioning, dilution, and chemical aging of semivolatile organics., *Environ. Sci. Technol.*, 40, 2635–43, 2006.
- Donahue, N. M., Epstein, S. A., Pandis, S. N., and Robinson, A. L.: A two-dimensional volatility basis set: 1. organic-aerosol mixing thermodynamics, *Atmos. Chem. Phys.*, 11, 3303–3318, 2011.
- Donahue, N. M., Henry, K. M., Mentel, T. F., Kiendler-Scharr, A., Spindler, C., Bohn, B., Brauers, T., Dorn, H. P., Fuchs, H., Tillmann, R., Wahner, A., Saathoff, H., Naumann, K.-H., Möhler, O., Leisner, T., Müller, L., Reinnig, M.-C., Hoffmann, T., Salo, K., Hallquist, M., Frosch, M., Bilde, M., Tritscher, T., Barmet, P., Praplan, A. P., DeCarlo, P. F., Dommen, J., Prévôt, A. S. H., and Baltensperger, U.: Aging of biogenic secondary organic aerosol via gas-phase OH radical reactions., *Proc. Natl. Acad. Sci. U. S. A.*, 109, 13503–8, 2012.
- Donahue, N. M., Chuang, W., Epstein, S. A., Kroll, J. H., Worsnop, D. R., Robinson, A. L., Adams, P. J., and Pandis, S. N.: Why do organic aerosols exist? Understanding aerosol lifetimes using the two-dimensional volatility basis set, *Environ. Chem.*, 10, 151, 2013.
- Donahue, N. M., Robinson, A. L., Trump, E. R., Riipinen, I., and Kroll, J. H.: Volatility and Aging of Atmospheric Organic Aerosol, *Top. Curr. Chem.*, 2014.
- Elrod, M. J.: Kinetics study of the aromatic bicyclic peroxy radical + NO reaction: overall rate constant and nitrate product yield measurements., *J. Phys. Chem. A.*, 115, 8125–30, 2011.
- Farmer, D. K., Matsunaga, A., Docherty, K. S., Surratt, J. D., Seinfeld, J. H., Ziemann, P. J., and Jimenez, J. L.: Response of an aerosol mass spectrometer to organonitrates and organosulfates and implications for atmospheric chemistry, *Proc. Natl. Acad. Sci. U. S. A.*, 107, 6670–6675, 2010.
- Fry, J. L., Draper, D. C., Zarzana, K. J., Campuzano-Jost, P., Day, D. a., Jimenez, J. L., Brown, S. S., Cohen, R. C., Kaser, L., Hansel, A., Cappellin, L., Karl, T., Hodzic Roux, A., Turnipseed, A., Cantrell, C., Lefer, B. L., and Grossberg, N.: Observations of gas- and aerosol-phase organic nitrates at BEACHON-RoMBAS 2011, *Atmos. Chem. Phys.*, 13, 8585–8605, 2013.
- Garnes, L. A. and Allen, D. T.: Size Distributions of Organonitrates in Ambient Aerosol Collected in Houston, Texas, *Aerosol Sci. Technol.*, 36, 983–992, 2002.
- Goldstein, A. H. and Galbally, I. E.: Known and Unexplored Organic Constituents in the Earth's Atmosphere, *Environ. Sci. Technol.*, 41, 1514–1521, 2007.
- Hallquist, M., Wenger, J. C., Baltensperger, U., Rudich, Y., Simpson, D., Claeys, M., and Dommen, J.: The formation, properties and impact of secondary organic aerosol: current and emerging issues, *Atmos. Chem. Phys.*, 9, 5155–5236, 2009.
- He, Q.-f., Ding, X., Wang, X.-m., Yu, J.-z., Fu, X.-x., and Liu, T.-y.: Organosulfates from Pinene and Isoprene over the Pearl River Delta, South China: Seasonal Variation and Implication in Formation Mechanisms, *Environ. Sci. Technol.*, 2014.
- Henry, K. M. and Donahue, N. M.: Photochemical aging of  $\alpha$ -pinene secondary organic aerosol: effects of OH radical sources and photolysis., *J. Phys. Chem. A*, 116, 5932–5940, 2012.
- Jimenez, J. L., Canagaratna, M. R., Donahue, N. M., Prévôt, A. S. H., Zhang, Q., Kroll, J. H., DeCarlo, P. F., Allan, J. D., Coe, H., Ng, N. L., Aiken, A. C., Docherty, K. S., Ulbrich, I. M., Grieshop, A. P., Robinson, A. L., Duplissy, J., Smith, J. D., Wilson, K. R., Lanz, V. A., Hueglin, C., Sun, Y. L., Tian, J., Laaksonen, A., Raatikainen, T., Rautiainen, J., Vaattovaara, P., Ehn, M., Kulmala, M., Tomlinson, J. M., Collins, D. R., Cubison, M. J., Dunlea, E. J., Huffman, J. A., Onasch, T. B., Alfarra, M. R., Williams, P. I., Bower, K., Kondo, Y., Schneider, J., Drewnick, F., Borrmann, S., Weimer, S., Demerjian, K., Salcedo, D., Cottrell, L., Griffin, R., Takami, A., Miyoshi, T., Hatakeyama, S., Shimono, A., Sun, J. Y., Zhang, Y. M., Dzepina, K., Kimmel, J. R., Sueper, D., Jayne, J. T., Herndon, S. C., Trimborn, A. M., Williams, L. R., Wood, E. C., Middlebrook, A. M., Kolb, C. E., Baltensperger, U., and Worsnop, D. R.: Evolution of organic aerosols in the atmosphere., *Science (80-. )*, 326, 1525–1529, 2009.
- Kalberer, M., Paulsen, D., Sax, M., Steinbacher, M., Dommen, J., Prévôt, A. S. H., Fisseha, R., Weingartner, E., Frankevich, V., Zenobi, R., and Baltensperger, U.: Identification of Polymers as Major Components of Atmospheric Organic Aerosols, *Science (80-. )*, 303, 1659–1662, 2004.
- Kanakidou, M., Seinfeld, J. H., Pandis, S. N., Barnes, I., Dentener, F. J., Facchini, M. C., Van Dingenen, R., Ervens, B., Nenes, A., Nielsen, C. J., Swietlicki, E., Putaud, J. P., Balkanski, Y., Fuzzi, S., Horth, J., Moortgat, G. K., Winterhalter, R., Myhre, C. E. L., Tsigaridis, K., Vignati, E., Stephanou, E. G., and Wilson, J. C.: Organic aerosol and global climate modelling: a review, *Atmos. Chem. Phys.*, 5, 1053–1123, 2005.
- Kroll, J. H., Ng, N. L., Murphy, S. M., Flagan, R. C., and Seinfeld, J. H.: Secondary organic aerosol formation from isoprene photooxidation., *Environ. Sci. Technol.*, 40, 1869–1877, 2006.
- Kroll, J. H., Smith, J. D., Che, D. L., Kessler, S. H., Worsnop, D. R., and Wilson, K. R.: Physical chemistry of aerosols., *Phys. Chem. Chem. Phys.*, 11, 8007–8014, 2009.

- Kroll, J. H., Donahue, N. M., Jimenez, J. L., Kessler, S. H., Canagaratna, M. R., Wilson, K. R., Altieri, K. E., Mazzoleni, L. R., Wozniak, A. S., Bluhm, H., Mysak, E. R., Smith, J. D., Kolb, C. E., and Worsnop, D. R.: Carbon oxidation state as a metric for describing the chemistry of atmospheric organic aerosol., *Nat. Chem.*, 3, 133–139, 2011.
- Kwok, E. S. C. and Atkinson, R.: Estimation Of Hydroxyl Radical Reaction Rate Constants For Gas-Phase Organic Compounds Using A Structure-Reactivity Relationship: An Update, *Atmos. Environ.*, 29, 1685–1695, 1995.
- Lane, T. E., Donahue, N. M., and Pandis, S. N.: Simulating secondary organic aerosol formation using the volatility basis-set approach in a chemical transport model, *Atmos. Environ.*, 42, 7439–7451, 2008a.
- Lane, T. E., Donahue, N. M., and Pandis, S. N.: Effect of NO<sub>x</sub> on Secondary Organic Aerosol Concentrations, *Environ. Sci. Technol.*, 42, 6022–6027, 2008b.
- Lim, Y. B. and Ziemann, P. J.: Effects of molecular structure on aerosol yields from OH radical-initiated reactions of linear, branched, and cyclic alkanes in the presence of NO<sub>x</sub>., *Environ. Sci. Technol.*, 43, 2328–34, 2009.
- Liu, S., Shilling, J. E., Song, C., Hiranuma, N., Zaveri, R. A., and Russell, L. M.: Hydrolysis of Organonitrate Functional Groups in Aerosol Particles, *Aerosol Sci. Technol.*, 46, 1359–1369, 2012.
- Logan, J. A., Prather, M. J., Wofsy, S. C., and McElroy, M. B.: Tropospheric chemistry: A global perspective, *J. Geophys. Res.*, 86, 7210–7254, 1981.
- Minguillón, M. C., Perron, N., Querol, X., Szidat, S., Fahrni, S. M., Alastuey, A., Jimenez, J. L., Mohr, C., Ortega, A. M., Day, D. A., Lanz, V. A., Wacker, L., Reche, C., Cusack, M., Amato, F., Kiss, G., Hoffer, A., Decesari, S., Moretti, F., Hillamo, R., Teinilä, K., Seco, R., Pemñuelas, J., Metzger, A., Schallhart, S., Müller, M., Hansel, A., Burkhardt, J. F., Baltensperger, U., and Prévôt, A. S. H.: Fossil versus contemporary sources of fine elemental and organic carbonaceous particulate matter during the DAURE campaign in Northeast Spain, *Atmos. Chem. Phys.*, 11, 12 067–12 084, 2011.
- Murphy, B. N., Donahue, N. M., Fountoukis, C., Dall’Osto, M., O’Dowd, C., Kiendler-Scharr, A., and Pandis, S. N.: Functionalization and fragmentation during ambient organic aerosol aging: application of the 2-D volatility basis set to field studies, *Atmos. Chem. Phys.*, 12, 10 797–10 816, 2012.
- Murphy, B. N., Donahue, N. M., Robinson, A. L., and Pandis, S. N.: A naming convention for atmospheric organic aerosol, *Atmos. Chem. Phys.*, 14, 5825–5839, 2014.
- Mylonas, D. T., Allen, D. T., Ehrman, S. H., and Pratsinis, S. E.: The Sources And Size Distributions Of Organonitrates In Los Angeles Aerosol, *Atmos. Environ.*, 25A, 2855–2861, 1991.
- Ng, N. L., Chhabra, P. S., Chan, A. W. H., Surratt, J. D., Kroll, J. H., Kwan, A. J., McCabe, D. C., Wennberg, P. O., Sorooshian, A., Murphy, S. M., Dalleska, N. F., Flagan, R. C., and Seinfeld, J. H.: Effect of NO<sub>x</sub> level on secondary organic aerosol (SOA) formation from the photooxidation of terpenes, *Atmos. Chem. Phys.*, 7, 5159–5174, 2007.
- Odum, J. R., Hoffmann, T., Bowman, F., Collins, D., Flagan, R. C., and Seinfeld, J. H.: Gas/Particle Partitioning and Secondary Organic Aerosol Yields, *Environ. Sci. Technol.*, 30, 2580–2585, 1996.
- Pandis, S. N., Paulson, S. E., Seinfeld, J. H., and Flagan, R. C.: Aerosol Formation in the Photooxidation of Isoprene and  $\beta$ -Pinene, *Atmos. Environ.*, 25, 997–1008, 1991.
- Pankow, J. F.: An Absorption Model Of The Gas / Aerosol Partitioning Involved In The Formation Of Secondary Organic Aerosol, *Atmos. Environ.*, 28, 189–193, 1994.
- Pankow, J. F. and Asher, W. E.: SIMPOL.1: a simple group contribution method for predicting vapor pressures and enthalpies of vaporization of multifunctional organic compounds, *Atmos. Chem. Phys.*, 8, 2773–2796, 2008.
- Pathak, R. K., Presto, A. A., Lane, T. E., Stanier, C. O., Donahue, N. M., and Pandis, S. N.: Ozonolysis of  $\alpha$ -pinene: parameterization of secondary organic aerosol mass fraction, *Atmos. Chem. Phys.*, 7, 3811–3821, 2007.
- Peng, R. D., Dominici, F., Pastor-Barriuso, R., Zeger, S. L., and Samet, J. M.: Seasonal analyses of air pollution and mortality in 100 US cities, *Am. J. Epidemiol.*, 161, 585–594, 2005.
- Pope, C. A., Ezzati, M., and Dockery, D. W.: Fine-Particulate Air Pollution and Life Expectancy in the United States, *N. Engl. J. Med.*, 360, 376–386, 2009.
- Presto, A. A. and Donahue, N. M.: Investigation of alpha-pinene + ozone secondary organic aerosol formation at low total aerosol mass., *Environ. Sci. Technol.*, 40, 3536–3543, 2006.
- Presto, A. A., Hartz, K. E. H., and Donahue, N. M.: Secondary organic aerosol production from terpene ozonolysis. 2. Effect of NO<sub>x</sub> concentration., *Environ. Sci. Technol.*, 39, 7046–54, 2005.
- Rollins, A. W., Kiendler-Scharr, A., Fry, J., Brauers, T., Brown, S. S., Dorn, H.-P., Dubé, W. P., Fuchs, H., Mensah, A., Mentel, T. F., Rohrer, F., Tillmann, R., Wegener, R., Wooldridge, P. J., and Cohen, R. C.: Isoprene oxidation by nitrate radical: alkyl nitrate and secondary organic aerosol yields, *Atmos. Chem. Phys.*, 9, 6685–6703, 2009.
- Rollins, A. W., Fry, J. L., Hunter, J. F., Kroll, J. H., Worsnop, D. R., Singaram, S. W., and Cohen, R. C.: Elemental analysis of aerosol organic nitrates with electron ionization high-resolution mass spectrometry, *Atmos. Meas. Tech.*, 3, 301–310, 2010.
- Russell, A. R., Valin, L. C., and Cohen, R. C.: Trends in OMI NO<sub>2</sub> observations over the US: effects of emission control technology and the economic recession, *Atmos. Chem. Phys. Discuss.*, 12, 12 197–12 209, 2012.
- Russell, L. M., Bahadur, R., and Ziemann, P. J.: Identifying organic aerosol sources by comparing functional group composition in chamber and atmospheric particles., *Proc. Natl. Acad. Sci. U. S. A.*, 108, 3516–21, 2011.
- Seinfeld, J. H. and Pandis, S. N.: *Atmospheric Chemistry and Physics: From Air Pollution to Climate Change*, Second Edition, John Wiley & Sons, Inc., 2006.
- Shilling, J. E., Chen, Q., King, S. M., Rosenoern, T., Kroll, J. H., Worsnop, D. R., DeCarlo, P. F., and Aiken, A. C.: Loading-dependent elemental composition of  $\alpha$ -pinene SOA particles, *Atmos. Chem. Phys.*, 9, 771–782, 2009.
- Shilling, J. E., Zaveri, R. A., Fast, J. D., Kleinman, L., Alexander, M. L., Canagaratna, M. R., Fortner, E., Hubbe, J. M., Jayne, J. T., Sedlacek, A., Setyan, A., Springston, S., Worsnop, D. R., and Zhang, Q.: Enhanced SOA formation from mixed anthropogenic and biogenic emissions during the CARES campaign, *Atmos. Chem. Phys.*, 13, 2091–2113, 2013.
- Shrivastava, M. K., Lane, T. E., Donahue, N. M., Pandis, S. N., and Robinson, A. L.: Effects of gas particle partitioning and aging of



- primary emissions on urban and regional organic aerosol concentrations, *J. Geophys. Res.*, 113, D18 301, 2008.
- Spracklen, D. V., Jimenez, J. L., Carslaw, K. S., Worsnop, D. R., Evans, M. J., Mann, G. W., Zhang, Q., Canagaratna, M. R., Allan, J., Coe, H., McFiggans, G., Rap, A., and Forster, P.: Aerosol mass spectrometer constraint on the global secondary organic aerosol budget, *Atmos. Chem. Phys.*, 11, 12 109–12 136, 2011.
- Thompson, A. M. and Cicerone, R. J.: Clouds and Wet Removal as Causes of Variability in the Trace-Gas Composition of the Marine Troposphere, *J. Geophys. Res.*, 87, 8811–8826, 1982.
- Trump, E. R. and Donahue, N. M.: Oligomer formation within secondary organic aerosols: equilibrium and dynamic considerations, *Atmos. Chem. Phys.*, 14, 3691–3701, 2014.
- Trump, E. R., Riipinen, I., and Donahue, N. M.: Interactions between atmospheric ultrafine particles and secondary organic aerosol mass : a model study, *Boreal Environ. Res.*, 19, 352–362, 2014.
- Turpin, B. J. and Huntzicker, J. J.: Identification Of Secondary Organic Aerosol Episodes And Quantitation Of Primary And Secondary Organic Aerosol Concentrations During SCAQS, *Atmos. Environ.*, 29, 3527–3544, 1995.
- Turpin, B. J., Saxena, P., and Andrews, E.: Measuring and simulating particulate organics in the atmosphere: problems and prospects, *Atmos. Environ.*, 34, 2983–3013, 2000.
- Weber, R. J., Sullivan, A. P., Peltier, R. E., Russell, A., Yan, B., Zheng, M., de Gouw, J., Warneke, C., Brock, C., Holloway, J. S., Atlas, E. L., and Edgerton, E.: A study of secondary organic aerosol formation in the anthropogenic-influenced southeastern United States, *J. Geophys. Res.*, 112, 1–13, 2007.
- Wittig, A. E., Anderson, N., Khlystov, A. Y., Pandis, S. N., Davidson, C. I., and Robinson, A. L.: Pittsburgh air quality study overview, *Atmos. Environ.*, 38, 3107–3125, 2004.
- Yeh, G. K. and Ziemann, P. J.: Alkyl Nitrate Formation from the Reactions of C8 - C14 n-Alkanes with OH Radicals in the Presence of NO: Measured Yields with Essential Corrections for Gas-Wall Partitioning, *J. Phys. Chem. A.*, 118, 8797–8806, 2014.
- Zhang, J., Dransfield, T., and Donahue, N. M.: On the Mechanism for Nitrate Formation via the Peroxy Radical + NO Reaction, *J. Phys. Chem. A*, 108, 9082–9095, 2004.
- Zhang, J., Huff Hartz, K. E., Pandis, S. N., and Donahue, N. M.: Secondary organic aerosol formation from limonene ozonolysis: homogeneous and heterogeneous influences as a function of NOx., *J. Phys. Chem. A.*, 110, 11 053–11 063, 2006.
- Zhang, Q., Jimenez, J. L., Canagaratna, M. R., Allan, J. D., Coe, H., Ulbrich, I., Alfarra, M. R., Takami, A., Middlebrook, a. M., Sun, Y. L., Dzepina, K., Dunlea, E., Docherty, K., DeCarlo, P. F., Salcedo, D., Onasch, T., Jayne, J. T., Miyoshi, T., Shimo, A., Hatakeyama, S., Takegawa, N., Kondo, Y., Schneider, J., Drewnick, F., Borrmann, S., Weimer, S., Demerjian, K., Williams, P., Bower, K., Bahreini, R., Cottrell, L., Griffin, R. J., Rautiainen, J., Sun, J. Y., Zhang, Y. M., and Worsnop, D. R.: Ubiquity and dominance of oxygenated species in organic aerosols in anthropogenically-influenced Northern Hemisphere midlatitudes, *Geophys. Res. Lett.*, 34, L13 801, 2007.
- Zhang, Y. L., Perron, N., Ciobanu, V. G., Zotter, P., Minguilón, M. C., Wacker, L., Prévôt, A. S. H., Baltensperger, U., and Szidat, S.: On the isolation of OC and EC and the optimal strategy of radiocarbon-based source apportionment of carbonaceous aerosols, *Atmos. Chem. Phys.*, 12, 10 841–10 856, 2012.
- Ziemann, P. J. and Atkinson, R.: Kinetics, products, and mechanisms of secondary organic aerosol formation., *Chem. Soc. Rev.*, 41, 6582–6605, 2012.